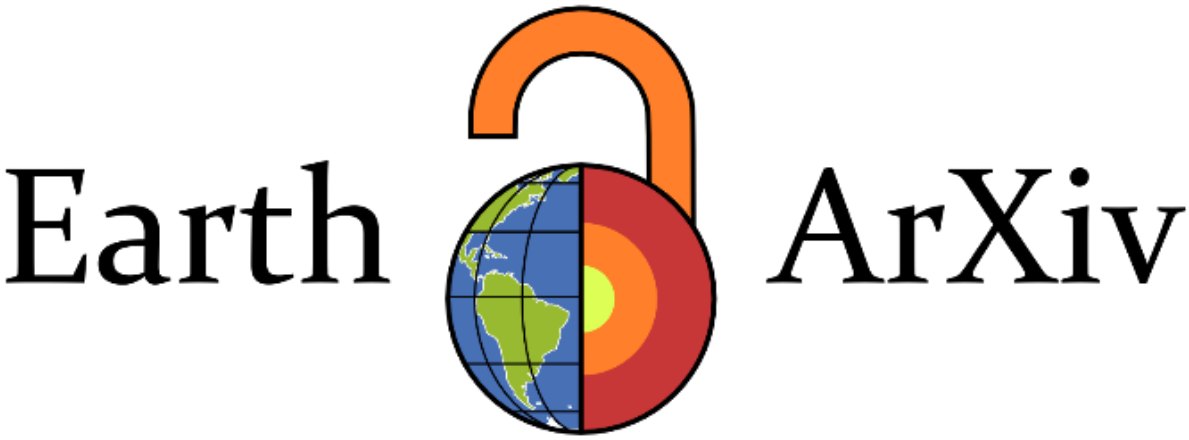

Bacterial tetraether lipid biosynthesis links membrane adaption to paleoclimate proxies

Vivien Schneider[1]*, Catherine G. Fontana[3], Adam D. Younkin[3], Ashley J. Winter[2], Felix J. Elling[4], Sebastian H. Kopf[3], and B. David. A. Naafs[1]

[1]Organic Geochemistry Unit (OGU), School of Chemistry, University of Bristol, UK
[2]School of Chemistry, University of Bristol, UK
[3]Department of Earth Sciences, University of Colorado Boulder, USA
[4]Institute of Earth Sciences, Heidelberg University, Germany

*Corresponding author vivien.schneider@bristol.ac.uk

Abstract

Membrane-spanning tetraether lipids are best known as an adaptive mechanism of archaea for stabilizing their membranes under extreme conditions. Bacteria typically rely on bilayer-forming phospholipids, making the occurrence of membrane-spanning branched glycerol dialkyl glycerol tetraethers (brGDGTs) in some bacteria highly unusual. BrGDGTs occur globally in soils and sediments and exhibit systematic structural changes (degree of methylation) with temperature, forming the basis of widely used paleoclimate proxies. However, their biosynthetic pathway has remained largely unresolved. Here, we conducted isotope-labeling experiments with *Solibacter usitatus* to elucidate brGDGT biosynthesis. Our results demonstrate that L-Leucine supplies the *iso*-branched building blocks of brGDGT alkyl chains via *iso*$C_{15:0}$ fatty acids and *iso*$C_{15:0}$ dialkyl glycerol diether intermediates, and that L-methionine provides the methyl group for additional chain methylation, with a labeling pattern implicating a class B radical S-adenosylmethionine methyltransferase. These findings establish a mechanistic understanding for bacterial tetraether biosynthesis that underpins paleoclimate proxies and reveal how bacteria modify membrane lipids, showing similarities across the Domains of Life.

Teaser

Elucidating the biosynthesis of brGDGTs and their structural changes provides a biological foundation for widely used terrestrial temperature proxy.

Introduction

Lipids are an essential part of an organism's cell membrane and subject to constant changes in relation to external stressors such as temperature, oxygen, and/or pH (*1*). Glycerol Dialkyl Glycerol Tetraethers (GDGTs) are a type of membrane-spanning lipids that are of particular interest as these lipids are ubiquitous in the environment and preserved on geological time scales in sedimentary archives. Their distribution is controlled by environmental parameters such as temperature, forming the basis for different paleothermometers (*2-4*). For example, a significant portion of our understanding of the operation of Earth's climate over the past ~100 Myrs is based on GDGTs (*5-9*).

Although most GDGTs are synthesized by archaea (*10*), some GDGTs are produced by bacteria (*11-13*), but their chemical structure is distinctively different. Archaea synthesize GDGTs composed of isoprenoidal alkyl chains (*iso*GDGTs), whereas bacteria produce GDGTs with branched (non-isoprenoid) alkyl chains (brGDGTs); both are ether linked to a glycerol backbone, although their stereochemistry is opposite. *iso*GDGTs have a 2,3-di-O-alkyl-*sn*-glycerol stereochemistry, whereas bacteria 1,2-di-O-alkyl-*sn*-glycerol for the linkage between their alkyl chains to the glycerol backbone (*14*). BrGDGTs mainly exist as tetra-, penta-, and hexamethylated homologues with the relative abundance between these brGDGTs depending on environmental constraints such as temperature in both the environment (mineral soils, peats, and lakes) and culture studies (*3, 4, 15-17, 12*). The discovery of brGDGTs being part of bacterial cell membranes challenged the lipid divide theory, which traditionally assumed that archaea synthesize ether-linked lipids consisting of a glycerol 1-phosphate which are often membrane-spanning, whereas bacteria normally biosynthesize ester-linked lipids with a glycerol 3-phosphate backbone forming a bilayer lipid structure of the cell membrane (*18*). Therefore, brGDGTs are relevant to diverse research directions: evolution of lipid biosynthesis, the transfer of the genetic capability to synthesize membrane-spanning lipids between the Domains of Life, the biosynthetic pathway of these lipids and their alteration in response to environmental change which subsequently is fundamental for their application as paleothermometers.

However, although recent advances have elucidated the full biosynthetic pathway of archaeal *iso*GDGTs (*19*), key aspects of the biosynthetic pathway leading to the formation of bacterial brGDGTs remain speculative and subject to major debate in the literature (*11, 20, 13, 21, 22*). Specifically, the key molecular building blocks that are used in brGDGT biosynthesis as well as the mechanism driving additional methylations in the chains of brGDGTs is unknown. Due to this knowledge gap, we do not understand the ecological and evolutionary significance of these lipids, nor the way bacteria obtained the capacity to synthesize membrane-spanning ether lipids, neither the biological mechanisms underpinning the widely used terrestrial paleothermometer. Here, we solve this conundrum by reporting results from culture experiments with the bacterium *Solibacter usitatus* Ellin6076, currently the only isolated organism to biosynthesize brGDGTs with additional methyl groups as well as cyclopentane rings in the alkyl chains (*12, 13*). Using isotopically labeled substrates, we demonstrate that in *S. usitatus*, *iso*$C_{15:0}$ fatty acids (FAs) and *iso*$C_{15:0}$ dialkyl glycerol diether (DEGs) are key intermediates in the biosynthesis of brGDGTs. We subsequently show that in this bacterium L-methionine provides the methyl group for penta- and hexamethylated brGDGTs. Based on our results, we conclude that the mechanism behind the additional methylation at C5 in brGDGTs is mediated by a class B radical SAM methyltransferase. Our results solve the long-standing debate regarding the biosynthetic pathway of brGDGTs and examined bacterial adaptation to environmental stress by modifying their membrane-spanning lipids.

Results

We performed a range of culture experiments with the bacterium *S. usitatus* at the University of Colorado Boulder. We cultured *S. usitatus* with 5,5,5-D_3 L-Leucine to elucidate the key biosynthetic intermediates in brGDGT production, specifically focusing on the debate whether *iso*$C_{15:0}$ DEG (and brGDDs) or *iso*-diabolic acid (*iso*-DA) are intermediates in brGDGT biosynthesis and the relative timing of the ester/ether conversion. This is followed by culture experiments with deuterated (methyl-CD_3) L-methionine to determine the origin of the additional methyl groups in penta-and hexamethylated brGDGTs and elucidate the mechanism driving them, while also determining the relative timing of the addition of methyl group.

BrGDGT production using L-Leucine shows that *iso*$C_{15:0}$ FA, *iso*$C_{15:0}$ DEG, and brGTGT serve as intermediates

S. usitatus was cultured with 5,5,5-D_3 L-Leucine, after which the lipid composition was analyzed to determine whether the label had been incorporated in brGDGTs, as well as other lipids as potential intermediates. Under our culture conditions, *S. usitatus* produced a range of lipids including branched, saturated-, and straight chain fatty acids (FAs) spanning C_{14} to C_{22} FAs, *iso*$C_{15:0}$ DEG as the dominant diether and trace amounts of *iso*$C_{16:0}$ DEG, as well as the membrane-spanning tetraether lipids brGTGT-Ia (featuring two dimerized alkyl chains from a DEG, with the other two remaining separate), brGDGT-Ia, -IIa, -IIIa, -Ib and -IIb, as well as brGDD-Ia, -IIa, and -IIIa (lipids that miss one of the two glycerols, see Fig. S1, S2 and Table S1). This lipid profile is consistent with that reported in non-labeled culture studies for this bacterium (11-13).

Importantly, our results demonstrate the incorporation of the deuterated methyl group (CD_3) from L-Leucine in *iso*$C_{15:0}$ FA (as well as *iso*$C_{17:0}$ FA), *iso*$C_{15:0}$ DEG, and brGTGTs and brGDGTs. We detect no label incorporation into the straight chain FAs. For the *iso*$C_{15:0}$ FA the expected mass shift of +3 amu due to the deuterated methyl group was identified for the molecular ion and observed in the fragmentation pattern from the gas chromatography-mass spectrometry (GC-MS) analysis (Fig. 1). A subsequent mass shift of +6 amu was observed for the $[M+H]^+$, $[M+NH_4]^+$ and $[M+Na]^+$ ions of the *iso*$C_{15:0}$ DEG in our liquid-chromatography-mass spectrometer (LC-MS) analysis (Fig. 2A, C and Fig. S3). Furthermore, the $[M+H]^+$, $[M+NH_4]^+$ and $[M+Na]^+$ ions showed mass shifts between +3 up to +12 amu (predominantly in the +8 to +12 amu range) for brGDGTs (Fig. 2B, D and Fig. S4), brGTGT-Ia, as well as brGDDs. These data confirm L-Leucine as the crucial amino acid in brGDGT biosynthesis and show *iso*$C_{15:0}$ FA, *iso*$C_{15:0}$ DEG, and brGTGT-Ia as key intermediates in the biosynthetic pathway of brGDGTs in *S. usitatus*, as well as constraining that the ester-ether conversion occurs likely at the stage of diester to diether lipids.

Methylation of penta- and hexamethylated brGDGTs via L-methionine

In additional experiments, we incubated *S. usitatus* with deuterated L-methionine (methyl-D_3) to determine the origin and mechanism driving the additional methylation in penta- and hexamethylated brGDGTs, and hence constrain the biological basis for the temperature-dependent degree of methylation and basis of the widely used paleothermometer. In these experiments we observed no label uptake in any of the FAs (Fig. S5) nor DEG lipids, including *iso*$C_{15:0}$ FA and *iso*$C_{15:0}$ DEG. We also detect no label uptake for brGTGT-Ia nor brGDGT-Ia. However, label incorporation was observed for brGDGT-IIa, as well as brGDD-IIa by a mass shift of +3 amu in the L-methionine experiment in comparison to the control experiment (Fig. 3). To determine the exact position of the additional methyl group in the *n*-alkyl chain of brGDGT-IIa, the lipid extract was ether cleaved and the resulting alkyl chains analyzed by GC-MS. Based on the fragmentation pattern of alkyl chains from (methyl-CD_3) L-methionine-spiked cultures in the GC-MS measurements, the position of the additional methyl group in brGDGT-IIa was constrained to be

at the C5 position based on the specific fragments at *m/z* 88 and 270 (Fig. S6). These data highlight the mechanisms driving methylation as bacterial adaptation as well as the relative timing of this modification in the overall biosynthesis pathway of brGDGTs.

Discussion

Biosynthetic pathway of brGDGTs

The incorporation of the deuterated methyl group from CD_3 L-Leucine in *iso*$C_{15:0}$ FA, *iso*$C_{15:0}$ DEGs, brGTGTs, brGDGTs, and brGDDs conclusively demonstrates the full biosynthetic pathway of brGDGTs in *S. usitatus* (Fig. 4). Furthermore, it shows that brGDGT synthesis follows the *iso*-branched fatty acid biosynthesis pathway starting from L-Leucine (*23, 24*). The deuterated methyl group introduced in our spiked culture experiments is conserved throughout the fatty acid elongation cycle into branched chain fatty acids, ultimately appearing at either the iso-branched or terminal (bridging) methyl position because of the new stereocenter at C4 in L-Leucine when swapping hydrogen against deuterium. The same observations hold for other iso-branched FAs, such as *iso*$C_{17:0}$ FA, but these are present in much lower concentrations in our experiments. In the spiked experiment, ~98% of the *iso*$C_{15:0}$ FAs were labeled, leaving only a minor unlabeled fraction (Fig. AB). Given that CD_3 L-Leucine was added at OD_{600} ~0.05 and cells were harvested at OD_{600} ~0.35, label incorporation into approximately 85% ((0.35-0.05)/0.35) of the biomass would be expected. The higher observed incorporation (98%) suggests extensive turnover of the *iso*$C_{15:0}$ FA pool, indicating that pre-existing *iso*$C_{15:0}$ FAs were converted into other lipids and/or remodeled during growth.

A key role for L-Leucine in the biosynthesis of *iso*-branched FAs in the bacterium *S. usitatus* is consistent with culture data across a wide range of bacteria (*23, 24*), however, its involvement in *iso*DEG synthesis, though suspected, has not previously been proven. Since *iso*DEGs are proposed to play a central role in the formation of brGDGTs, we explored the importance of L-Leucine in *iso*$C_{15:0}$ DEG formation and downstream lipid biosynthesis like brGDGTs.

The biosynthetic pathway of bacterial (*iso*-) DEGs is not well constrained, as DEGs are not common in bacteria (*25*), although they can be abundant in sedimentary archives and have been used as paleoclimate proxy (*26, 27*). Our results provide novel insights, showing L-Leucine label being incorporated into *iso*$C_{15:0}$ DEG (~99%). This demonstrates that two *iso*$C_{15:0}$ FAs form the basis of *iso*$C_{15:0}$ DEG, with the *iso*-branching from L-Leucine, also seen in the FAs, being preserved into the *iso*$C_{15:0}$ DEG. Moreover, we expand on that, showing that the methylation in *iso*-branched FAs and *iso*DEGs is based on the original amino acid-building block. The role of L-Leucine in bacterial *iso*DEG biosynthesis that we identify here is novel, but consistent with the findings in some halophilic archaea (*28, 29*) were L-Leucine forms the basis for the isoprenoid building block that leads to the formation of archaeal isoprenoidal DEGs such as archaeol (*28, 29*). In these archaea, L-Leucine is transformed into 3-hydroxy-3-methylglutaryl (HMG)-CoA and thus enters the mevalonate pathway, which subsequently leads to the formation of isoprenoids. The fact that we mainly observe *iso*$C_{15:0}$ DEGs with a mass shift of +6 amu (representing two deuterated methyl groups), in combination with a calculated label incorporation of ~99% indicates that the turn-over time of the *iso*$C_{15:0}$ DEGs was relatively high, similar as for *iso*$C_{15:0}$ FAs. In addition, the high percentage of label incorporation suggests that most unlabeled *iso*$C_{15:0}$ DEGs that existed at the time of label addition were remodeled into other lipids such as brGDGTs. This suggests that *iso*$C_{15:0}$ DEG are mostly an intermediate within brGDGT biosynthesis in this organism instead of occurring as individual membrane-lipids.

Lastly, we focus on membrane spanning tetraether lipids. We detect both brGTGTs, where only one of the long alkyl chains is dimerized, and brGDGTs. All these tetraethers lipids are labeled. Label incorporation from CD_3 L-Leucine in brGTGT-Ia was high at ~99%. BrGDGTs

show a spread of CD_3 L-Leucine label incorporation as evidenced by a range of mass shifts from +3 to +12 amu (mainly +8 to +12 amu) with around 64% (using [M+8 to +12] amu, Table S2) of brGDGTs showing label incorporation (Fig. 2C, D). This observed range of label incorporation can mostly be explained by the additional stereocenter at C4 in CD_3 L-Leucine (C13 in the precursor *iso*FA), the occurrence of isotopic homologues, as well as the inclusion of unlabeled *iso*FAs and/or *iso*DEGs into brGDGTs. The fact that we predominantly observe a mass shift of +8 to +12 amu indicates that the tail to tail coupling of two *iso*DEGs to form a brGDGT occurs through a Csp^3-Csp^3 bond formation as now confirmed for archaea (*19*) and not through coupling of unsaturated carbon bonds as suggested previously (*30*). Moreover, our results also indicate that brGDGTs have a longer turn-over-time compared to *iso*$C_{15:0}$ FAs, *iso*$C_{15:0}$ DEGs and brGTGTs. This longer turn-over time for brGDGTs in comparison to FAs seen in our culture experiments now provides a culture basis to explain similar observations from natural archives like peatlands (*31*). Furthermore, the decreasing percentage of label incorporation across different lipids elucidates the order of each biosynthetic step, specifically showing that brGTGTs are an intermediate towards brGDGT biosynthesis and not a degradation product. Label incorporation in brGDDs (~68%), lipids that lack one of the two glycerols, was between brGTGTs and brGDGTs. This observation demonstrates that brGDDs might be a another intermediate within the biosynthetic pathway of brGDGTs which would be in contrast to studies of archaeal *iso*GDDs, which are proposed to mainly represent degradation products (*32, 33*). However, the percentage difference of label incorporation of these brGDDs and brGDGTs is little and different ionization efficiencies during the analysis with LC-MS for these compounds have to be considered.

Overall and importantly, the incorporation of labeled L-Leucine into brGDGTs in combination with the decreasing percentage of label incorporation along the main steps within the biosynthetic pathway (Table S2) solves the long-standing conundrum regarding tetraether lipid biosynthesis by bacteria. Based on our results, we suggest that *iso*$C_{15:0}$ DEGs are the first ether lipid in the biosynthetic pathway of brGDGTs (*34*). In the next paragraph we discuss these findings into the context of the literature debate regarding brGDGT biosynthesis.

Following their discovery in the 1980s (*35*) and subsequent elucidation of their full chemical structure (*36*), the biosynthesis pathway that leads to the formation of bacterial tetraether lipids has been speculative and grouped in two competing hypotheses: one pathway focusing on DEGs as key-intermediate and the TetraEther Synthase (*Tes*) driving the coupling into membrane spanning lipids (*34, 13*), the other relying on *iso*-diabolic acid (*iso*-DA) as key intermediate and the Membrane-Spanning Synthase (*Mss*) driving the coupling (*37, 22*). Our data resolve this conundrum by demonstrating that in *S. usitatus*, brGDGT biosynthesis starts with L-Leucine, elongated to *iso*$C_{15:0}$ FA, two of which are combined and transformed from ester to ether to form an *iso*$C_{15:0}$ DEGs, of which two are subsequently partly combined leading to the formation of brGTGTs as intermediate before producing a tetra-methylated brGDGT through the dimerization of the other two *iso*$C_{15:0}$ FAs from the *iso*$C_{15:0}$ DEG. This biosynthesis pathway is analogous to that utilized by archaea, across the lipid divide, which use two archaeol diether lipids to biosynthesize *iso*GDGTs (*19*). Our results are inconsistent with the recently hypothesized pathway of brGDGT biosynthesis in which diesters are coupled to form tetraesters, which are then converted to tetraethers (*22*). Although, we can not rule out the possibility of a short-lived *iso*-DA intermediate, our results provide robust data to support the DEG pathway, at least in *S. usitatus,* currently the only known bacteria to biosynthesize the full range of brGDGTs (but no *iso*-DA). If other bacteria utilize the *iso*-DA (tetraester) pathway to produce brGDGTs, previous work demonstrates they also use L-Leucine as foundational amino-acid (*20*). However, the *iso*-DA (tetraester) pathway is so far not proven to lead to brGDGTs (*22*). Although *iso*-DA is synthesized by a wide range of (acido)bacteria (*11*), with one or two exceptions, none of these bacteria biosynthesize brGDGTs as part of their membrane (*37, 11, 22*). In addition, recent evidence from tropical peat cores shows that downcore variations in *iso*-DA concentrations are

not related to brGDGT concentrations from the same cores, while *iso*DEG and brGDGT concentrations show similar downcore trends, further suggesting that in nature, the DEG pathway as shown here for *S. usitatus* is likely dominant for brGDGT biosynthesis (*38*).So far, *S. usitatus* is the only known bacterium to synthesize all major brGDGTs, but cultures of two other acidobacteria contain traces of brGDGT-Ia; *Acidobacteriaceae* strain A2-4C and *E. aggregans* Wbg-1 (*37*). That other bacteria can synthesize brGDGTs is consistent with their global occurrence across different environments on the surface of the Earth (*36, 39, 34, 40-42*). Interestingly in the context of our findings, both *Acidobacteriaceae* and *E. aggregans* cultures also contain (low concentrations of the) *iso*$C_{15:0}$ DEG, suggesting that in these bacteria the DEG pathway could also be used for the biosynthesis of brGDGTs (*16, 13*).

With the full biosynthesis pathway of the tetramethylated brGDGT(-Ia) confirmed, we then explored the mechanism that leads to the formation of penta- and hexamethylated brGDGTs, lipids with one and two additional methyl groups, respectively. This is of particular importance as it is the relative abundance of these additionally methylated penta- and hexamethylated brGDGTs relative to tetramethylated brGDGT that underpins the terrestrial paleothermometer.

Methylation at C5 in pentamethylated brGDGTs

Our results from the deuterated L-methionine experiments for the first time show that the amino acid L-methionine acts as the methyl donor for the additional methylation at C5 in pentamethylated brGDGT-IIa (and -IIIa) in *S. usitatus*, currently the only known organisms to biosynthesize these lipids. It is the transfer of the adenosyl group from ATP to the sulfur atom of L-methionine during which a sulfonium ion is formed, which makes the methyl group nucleophilic and therefore facilities the transport of the methyl group from L-methionine to S-adenosyl-L-methionine (SAM). The amino acid L-methionine is known to acts as the methyl donor in a diverse range of methylation reactions, including for DNA, other membrane lipids and proteins (*43-46*), but was not known to be able to facilitate methylation of complex tetraether lipids in bacteria. Interestingly, L-methionine is thought to also act as methyl donor for the methylation of *iso*GDGTs in archaea (*43, 47*). Thus, our results indicate another similarity of pathways of lipid modification between the Domains of Archaea and Bacteria, further challenging the lipid divide theory and highlighting that microbial adaptation patterns are shared across Domains of Life.

Interestingly, we find no labelled nor unlabeled penta- nor hexamethylated brGTGTs. Only brGDGTs and brGDDs are penta- (and hexa)methylated and demonstrate L-methionine label uptake. These results further support our assessment that brGTGTs represent intermediates during brGDGT biosynthesis, while suggesting that brGDDs are likely a degradation products of brGDGTs, thus elucidating the complete order of biosynthesis of brGDGTs and constraining the timing of extra methylation to only occur on complete brGDGTs (Fig. 4, Fig. S9). Further studies still need to elucidate the mechanism behind the addition of cyclopentane moieties within brGDGTs, but based on our data we hypothesize that these will be introduced into the alkyl chain after a tetraether is formed, analogous to when methylations are added. We then explored the mechanism responsible for the methylation of brGDGTs, discussed below.

When determining the mechanisms underlying the methylation (*48*) at C5 in brGDGT-IIa, methionine dependent methyltransferase were excluded as potential enzymes responsible for brGDGT methylation since these enzymes methylate only sp^2 hybridized/aromatic carbons. To methylate sp^3 carbons as in brGDGT alkyl chains, these enzymes need an N-terminal cobalamin-binding domain (*49*). The other option is a radical SAM methyltransferase from class A, B, or C. To facilitate the methyltransfer on sp^2 carbons, enzymes from class A utilize two conserved cysteine residues. Currently, they are only known to conduct RNA methylations (*50, 51*) and are therefore unlikely to be responsible for the methylation the alkyl chains of brGDGTs. Class C

radical SAM methyltransferases utilize a 5'-dAdo* which abstracts one hydrogen (deuterium) from SAM to form a radical species (*51, 52*) which subsequently would have led to a mass shift of +2 amu instead of +3 amu as observed in our (methyl D_3) L-methionine labeling experiments. As our results confirmed a mass shift of +3 amu for the deuterated L-methionine experiments and since the carbons within the alkyl chain of brGDGTs are all sp^3 hybridized, we propose that a class B radical SAM methyltransferase is likely to be responsible for adding the methyl group at C5 in brGDGTs (Fig. 4) (*52*). In this scenario, the 5'-dAdo abstracts a hydrogen from the substrate which leads to the formation of a radical prior to the incorporation of the methyl group onto the substrate forming a new C-C bond (*49*). An involvement of methylcobalamin together with a radical SAM protein has been proposed to drive the methylation of archaeal *iso*GDGTs (*43, 47*). For isoprenoid Glycerol Monoalkyl Glycerol Tetraether (*iso*GMGTs) it was shown that a radical SAM protein named GMGT methylase (Gmm) is involved in the methylation of isoprenoidal alkyl chains (*47*). We propose that a similar mechanism drives the temperature-dependent methylation of brGDGTs in bacteria and hence the terrestrial temperature proxy. To further explore this, we performed a genomic comparison between *S. usitatus* and archaea.

Genomic comparison of methyltransferase in *S.usitatus* and archaea

When scanning the genome of *S. usitatus*, we found a total of 17 vitamin B12-binding radical SAM proteins with unknown function. Four of these (MiaB, RimO, HemW, HpnJ) can be assigned probable functions, leaving 13 uncharacterized proteins. Of these, 6 are likely class B methyltransferases: Acid_6623, Acid_6624, Acid_6625, Acid_6628, Acid_5781, Acid_5526. One of them, Acid_5781, occurs near a GDGT ring synthase (GrsA) homolog (Acid_5783), but not in the same operon or within immediate vicinity of tetraether synthase homologs (Tes; Acid_5929 or Acid_2410). We compared these six putative class B methyltransferases against Gmm, the radical SAM protein shown to methylate isoprenoidal tetraether lipids in archaea (*47*). The percentage identity between Gmm and our six candidate enzymes was low (23-29%) (Table S3). Although, most of our candidate enzymes show key features like a B12 and rSAM binding domain, their low sequence similarity is ambiguous since it was shown that unrelated B12-dependet rSAM enzymes often share significant sequence similarity up to ~30% (*53*). Due to the very limited number of brGDGT producing bacteria and *S. usitatus* being the only bacteria known to produce the full range of brGDGTs, a direct comparison between bacteria is not feasible at this moment. However once more brGDGT producing bacteria are identified a phylogenetic comparison might shed some light into the responsible enzymes.

Conclusions

This study conclusively elucidates the full biosynthetic pathway of brGDGT and the mechanism underlying structural modification (methylation) of these membrane lipids. We show that brGDGTs start with the amino acid L-leucine, which is used to form *iso*C_{15} FAs. These *iso*C_{15} FAs are then combined with a glycerol and reduced to DEGs. Two DEGs are then coupled to first form brGTGT-Ia and then brGDGT-Ia. Only once a tetraether is formed does the methylation at the C5 position occur using a type B radical SAM to form brGDGT-IIa. Our data demonstrate how bacteria biosynthesize the canonical brGDGTs and modify their membrane lipids depending on environmental stress, providing a biosynthetic basis for the widely used terrestrial paleothermometer.

Materials and Methods

Culturing

Solibacter usitatus Ellin6076 (DSM 22595) was acquired from the DSMZ (Deutsche Sammlung von Mikroorganismen und Zellkulturen GmbH). Cultivation was performed in modified DSMZ 1266 medium at 20°C, pH 5.5, and with 21% O_2. Cultures were incubated in darkness with shaking at 200 rpm and a total medium volume of 15 ml per culture replicate. The modified DSMZ medium 1266 consisted of 2.5 mM glucose, 0.2 mM KH_2PO_4, 0.27 mM $MgSO_4$, 0.4 mM $CaCl_2$, 13.3 mM 2-Morpholinoethanesulfonic acid (MES), 15 nM Na_2SeO_3,16 nM Na_2WO_4, 0.4 M NH_4Cl, 1.33 ml/l 10 trace element solution (2 mg/L $CuCl_2$, 190 mg/l $CoCl_2$, 1.5 g/l $FeCL_2$, 6 mg/l H_3BO_3, 100 mg/l $MnCl_2$, 36 mg/l Na_2MoO_4, 24 mg/l $NiCl_2$, 70 mg/l $ZnCL_2$), and 1.33 ml/l HS vitamin solution (50 mg/l alpha-lipoic acid (thioctic acid), 50 mg/l biotin (D+), 100 mg/l Ca-pantothenate (D+), 50 mg/l cyanocobalamin, 50 mg/l folic acid, 100 mg/l nicotinic acid (Niacin), 100 mg/l p/4-aminobenzoic acid, 100 mg/l pyridoxine hydrochloride, 100 mg/l riboflavin, 100 mg/l L-thiamine hydrochloride). To determine the growth rate, optical density (OD) measurements were taken using a GENESYS 30 visible spectrophotometer from Thermo Scientific. L-methionine-D_3 and L-Leucine-5,5,5-D_3 were purchased from Cambridge Isotope Laboratories and were added with a final concentration of 500 µM during early exponential growth at OD_{600} = 0.05 and harvested just before entering stationary phase at OD_{600} = 0.3 (Table S4-S5).

Lipid extraction

After the experiment, cells were harvested by centrifugation at 5000 rpm for 3 minutes and lyophilized overnight. Cell lysis was achieved using bead-beating with 0.1 µm glass beads in methanol, with methanol added to just cover the cells and beads. Samples were bead-beaten six times for 20 seconds, with a 10-minute cooling period after the first three cycles. Afterwards, samples were dried under a gentle stream of N_2. Acid hydrolysis of the cell extract was performed for 90 minutes at 65°C using 500 µl of 3M hydrochloric acid (36%) in methanol (MeOH), with a water content of 33% to cleave the head group and release ether core lipids, as well as transesterify fatty acids chains to fatty acid methyl esters (FAMEs). Next, 500 µl of methyl tert-butyl ether (MTBE) was added and samples were sonicated for 5 minutes, before being extracted three times using 500 µl hexane, whereby the upper organic layer was transferred and collected in a new vial representing the total lipid extract (TLE). The latter was dried under a gentle stream of N_2 before being filtered using a 0.45 µm PTFE filter using 100 µl of *n*-hexane:*iso*-propanol (99:1; *v/v*) and dried again.

Separation of the TLE into FAMEs and ether lipids

The TLE was redissolved in 250 µl ethyl acetate (EtoAC) and ~10% of the TLE was transferred into a new vial, whereas the other 90% was fractionated into FAMEs (F1) and ether lipids (F2) using a 500 mg aminopropyl column (Sigma Aldrich Discovery DSC-NH2). The column was conditioned with 6 ml of *n*-hexane, before the 90% of the TLE was transferred onto the column and F1 was eluted using *n*-hexane:dichlomethane (4:1; *v/v*) and F2 with 7 ml of dichloromethane:acetone (9:1; *v/v*). Both fractions were dried under N_2 before F1 was redissolved in cyclohexane and F2 in EtoAC.

Ether cleavage and hydrogenation

To determine the position of the methyl group in brGDGT-IIa, we performed ether cleavage on one half of F2 following the protocol from Rosendahl et al., 2026 (*54*). For this purpose, F2 was dissolved in 225 µl EtoAC, 112.5 µl were transferred into a new vial and dried under a gentle N_2 stream. 250 µl of hydroiodic acid (HI) was added and samples were incubated for 4 hours at 120°C. After 4 hours, samples were left for cooling before 250 µl HPLC-grade water was added

to neutralize the acid followed by and addition of 500 µl of *n*-hexane. The organic phase of the sample (alkyl iodides from cleaved ether lipids) was extracted three times; each time, samples were vortexed for 1 min before the upper *n*-hexane layer was transferred to a new vial. The combined *n*-hexane layers were dried under N_2. Then ~5 mg of platinum (IV) oxide (PtO_2), a magnetic stir bar and 1.5 ml of *n*-hexane was added, the vials were closed. Through the PTFE septum, a small stainless steel needle connected to a hydrogen (H_2) line was pierced and H_2 (<2 psi)) was bubbles through the samples for 90 minutes. After the hydrogenation finished, samples were dried under N_2 , before being resuspended in ~200 µl of *n*-hexane and filtered through glaswoll silica columns to remove PtO_2. To ensure complete transfer of all sample material, the glass vial and columns were rinsed three times.

Gas chromatography-mass spectrometry analysis of FAs from L-Leucine experiment

Prior to the analysis with gas chromatography-mass spectrometry (GC-MS), samples of F1 were derivatized with *N*$_2$*O*-Bis(trimethylsilyl)-trifluoroacetamide (BSTFA; 30 µl) and pyridine (25 µl) at 65°C for 1 hour. Samples were dried under a gentle stream of N_2 before being resuspended in EtoAC.

Samples were analyzed at the University of Bristol with a Trace 1310 gas chromatograph from Thermo Fisher Scientific coupled to an ISQ 7000 Quadrupole mass spectrometer and an Agilent HP-1 column (50 m x 0.32 mm; df 0.25 µm). A 1 µL aliquot of the sample was injected. The GC oven temperature was initially held at 70°C, then increased at 20°C/min to 130°C, followed by a ramp of 4°C/ min to 320°C, where it was held for 20 min. Helium was used as carrier gas at a constant flow rate of 2 ml/min. Mass spectra were continuously recorded over a *m/z* 50-650 range.

GC-MS analysis of ether cleaved brGDGTs from L-methionine experiment

Samples were analyzed at the University of Boulder, Colorado, USA, using a Thermo Scientific ISQ Single Quadrupole mass spectrometer and separated using a DB-5 column (30m x 0.25 mm; df 0.25 µm). The GC oven temperature started with 40°C for 2 min, before being increased to 295°C at 15°C/min, then to 315°C at 5°C/min, and finally to 375°C at 15°C/min with a final hold of 5 min. Helium was used as the carrier gas with a constant flow rate of 1.2 ml/min. Mass spectra were recorded over 50-750 *m/z*.

Liquid chromatography-mass spectrometry analysis of diether and tetraether lipids

For liquid chromatography-mass spectrometry (LC-MS) analysis, 10% of the TLE was used. Analyses were performed using a Thermo Scientific UltiMate 3000 UHPLC system coupled to a Thermo Scientific Orbitrap ID-X mass spectrometer. Compound separation was achieved using an Acquity UPLC C18 BEH column (2.1x 150 mm, 1.7 µm; Waters) maintained at 45°C. The system operated at a constant flow rate of 0.2 ml/min and 5 µl of each sample was injected for analysis.

The mobile phase consisted of two eluents; eluent A (MeOH: water, 85:15; *v/v*) and eluent B (MeOH:*iso*-propanol, 1:1; *v/v*). Both eluents contained 0.12% formic acid and 0.04% ammonium. The set-up of the mobile phase started with 5% B for the initial 3 min, followed by a continuous gradient reaching 50% at 12 min and then to 100% B at 50 min. The total run time was 80 min. Ionization was performed using a heated electrospray ionization (H-ESI) source operating in negative polarity mode. Source parameters were set as follows: sheath gas 25 arbitrary units (arb), auxiliary gas 10 arb, and sweep gas 4 arb. The ion transfer tube temperature was maintained at 300°C and the vaporizer temperature at 50°C. Data were acquired in full-scan mode over a *m/z* range of 500-1200. Data dependent analysis was performed using an intensity threshold of $\geq 2 \times 10^4$ ion and inclusion list, after which full-scan MS2 spectra were recorded over a *m/z* range of 200-1200. Analytes were identified using their protonated ($[M+H]^+$), ammoniated

([M+NH_4]$^+$) and sodiated mass ([M+Na]$^+$) in MS1, diagnostic fragmentation pattern in MS2, and elution pattern.

References

1. J. Šajbidor, Effect of Some Environmental Factors on the Content and Composition of Microbial Membrane Lipids. *Crit. Rev. Biotechnol.* **17**, 87-103 (1997).
2. S. Schouten, E. C. Hopmans, E. Schefuß, J. S. Sinninghe Damsté, Distributional variations in marine crenarchaeotal membrane lipids: a new tool for reconstructing ancient sea water temperatures? *EPSL* **204**, 265-274 (2002).
3. J. W. H. Weijers, S. Schouten, J. C. Van Den Donker, E. C. Hopmans, J. S. Sinninghe Damsté, Environmental controls on bacterial tetraether membrane lipid distribution in soils. *Geochim. Cosmochim. Acta* **71**, 703-713 (2007).
4. C. D. Jonge, E. C. Hopmans, C. I. Zell, J.-H. Kim, S. Schouten, J. S. Sinninghe Damsté, Occurrence and abundance of 6-methyl branched glycerol dialkyl glycerol tetraethers in soils: Implications for palaeoclimate reconstruction. *Geochim. Cosmochim. Acta* **141**, 97-112 (2014).
5. J. W. H. Weijers, S. Schouten, A. Sluijs, H. Brinkhuis, J. S. Sinninghe Damsté, Warm arctic continents during the Palaeocene–Eocene thermal maximum. *EPSL* **261**, 230-238 (2007).
6. B. D. A. Naafs, M. Rohrssen, G. N. Inglis, O. Lähteenoja, S. J. Feakins, M. E. Collinson, E. M. Kennedy, P. K. Singh, M. P. Singh, D. J. Lunt, R. D. Pancost, High temperatures in the terrestrial mid-latitudes during the early Palaeogene. *Nat. Geosci.* **11**, 766-771 (2018).
7. V. Lauretano, A. T. Kennedy-Asser, V. A. Korasidis, M. W. Wallace, P. J. Valdes, D. J. Lunt, R. D. Pancost, B. D. A. Naafs, Eocene to Oligocene terrestrial Southern Hemisphere cooling caused by declining pCO2. *Nat. Geosci.* **14**, 659-664 (2021).
8. R. Rattanasriampaipong, Y. G. Zhang, A. Pearson, B. P. Hedlund, S. Zhang, Archaeal lipids trace ecology and evolution of marine ammonia-oxidizing archaea. *Proc. Natl. Acad. Sci. USA* **119**, e2123193119 (2022).
9. E. J. Judd, J. E. Tierney, D. J. Lunt, I. P. Montañez, B. T. Huber, S. L. Wing, P. J. Valdes, A 485-million-year history of Earth's surface temperature. *Science* **385**, eadk3705 (2024).
10. Z. Zeng, H. Chen, H. Yang, Y. Chen, W. Yang, X. Feng, H. Pei, P. V. Welander, Identification of a protein responsible for the synthesis of archaeal membrane-spanning GDGT lipids. *Nat. Commun.* **13**, 1545 (2022).
11. J. S. Sinninghe Damsté, W. I. Rijpstra, E. C. Hopmans, J. W. Weijers, B. U. Foesel, J. Overmann, S. N. Dedysh, W. I. Rijpstra, An overview of the occurrence of ether- and ester-linked iso-diabolic acid membrane lipids in microbial cultures of the Acidobacteria: Implications for brGDGT paleoproxies for temperature and pH. *Org. Geochem.* **124**, 63-76 (2018).
12. Yufei Chen, Fengfeng Zheng, Huan Yang, Wei Yang, Ruijie Wu, Xinyu Liu, Huayang Liang, Huahui Chen, Hongye Pei, Chuanlun Zhang, Richard D. Pancost, Z. Zeng, The production of diverse brGDGTs by an Acidobacterium providing a physiological basis for paleoclimate proxies. *Geochim. Cosmochim. Acta* **337**, 155-165 (2022).
13. T. A. Halamka, J. H. Raberg, J. M. Mcfarlin, A. D. Younkin, C. Mulligan, X. L. Liu, S. H. Kopf, Production of diverse brGDGTs by Acidobacterium Solibacter usitatus in response to temperature, pH, and O2 provides a culturing perspective on brGDGT proxies and biosynthesis. *Geobiology* **21**, 102-118 (2023).
14. Y. Koga, Early evolution of membrane lipids: how did the lipid divide occur? *J Mol Evol* **72**, 274-282 (2011).
15. B. D. A. Naafs, G. N. Inglis, Y. Zheng, M. J. Amesbury, H. Biester, R. Bindlerf, J. Blewett, M. A. Burrows, D. Del Castillo Torres, F. M. Chambersi, A. D. Cohen, R. P. Evershed, S. J. Feakins, M. Gałka, A. Gallego-Sala, L. Gandois, D. M. Gray, P. G. Hatcher, E. N. Honorio Coronado, P. D. M. Hughes, A. Huguet, M. Könönen, F. Laggoun-Défarge, O. Lähteenoja, M. Lamentowicz, R. Marchant, E. Mcclymont, X. Pontevedra-Pombal, C. Ponton, A. Pourmand, A.M. Rizzuti, L. Rochefort, J. Schellekens, F. De Vleeschouwer, R. D. Pancost, Introducing global peat-specific temperature and pH calibrations based on brGDGT bacterial lipids. *Geochim. Cosmochim. Acta* **208**, 285-301 (2017).

16. T. A. Halamka, J. M. Mcfarlin, A. D. Younkin, J. Depoy, N. Dildar, S. H. Kopf, Oxygen limitation can trigger the production of branched GDGTs in culture. *Geochem. Perspect. Lett.*, 36-39 (2021).
17. P. Martínez-Sosa, J. E. Tierney, I. C. Stefanescu, E. Dearing Crampton-Flood, B. N. Shuman, C. Routson, A global Bayesian temperature calibration for lacustrine brGDGTs. *Geochim. Cosmochim. Acta* **305**, 87-105 (2021).
18. D. L. Valentine, Adaptations to energy stress dictate the ecology and evolution of the Archaea. *Nat. Rev. Microbiol.* **5**, 316-323 (2007).
19. C. T. Lloyd, D. F. Iwig, B. Wang, M. Cossu, W. W. Metcalf, A. K. Boal, S. J. Booker, Discovery, structure and mechanism of a tetraether lipid synthase. *Nature* **609**, 197-203 (2022).
20. D. X. Sahonero-Canavesi, M. F. Siliakus, A. Abdala Asbun, M. Koenen, F. a. B. Von Meijenfeldt, S. Boeren, N. J. Bale, J. C. Engelman, K. Fiege, L. Strack Van Schijndel, J. S. Sinninghe Damsté, L. Villanueva, Disentangling the lipid divide: Identification of key enzymes for the biosynthesis of membrane-spanning and ether lipids in Bacteria. *Sci Adv* **8**, (2022).
21. Y. Chen, H. Yang, F. Zheng, R. Wu, C. Zhang, B. D. A. Naafs, R. D. Pancost, Z. Zeng, Temperature-dependent modulation of the methylation degree of (tetra)ester-linked membrane-spanning lipids in an Acidobacterium. *Geochimica et Cosmochimica Acta* **401**, 190-203 (2025).
22. Diana X. Sahonero-Canavesi, Nicole J. Bale, Melissa Antony Venancius, Michel Koenen, E. C. Hopmans1, Jaap S. Sinninghe Damsté, L. Villanueva, Towards understanding the bacterial biosynthesis of branched GDGTs: Identification of iso-diabolic acid-based tetraester and mixed ether/ester, membrane-spanning lipid intermediates in members of the Bacillota *bioRxiv.*, (2026).
23. T. Kaneda, Iso- and anteiso-fatty acids in bacteria: biosynthesis, function, and taxonomic significance. *Microbiol. Rev.* **55**, 288-302 (1991).
24. M. W. Frank, S. G. Whaley, C. O. Rock, Branched-chain amino acid metabolism controls membrane phospholipid structure in Staphylococcus aureus. *J Biol Chem* **297**, 101255 (2021).
25. V. Grossi, D. Mollex, A. Vinçon-Laugier, F. Hakil, M. Pacton, C. Cravo-Laureau, Mono- and dialkyl glycerol ether lipids in anaerobic bacteria: Biosynthetic insights from the mesophilic sulfate reducer Desulfatibacillum alkenivorans PF2803T. *Appl. Environ. Microbiol* **81**, 3157-3168 (2015).
26. R. D. Pancost, I. Bouloubassi, G. Aloisi, J. S. Sinninghe Damsté, T. M. S. Scientific Party, Three series of non-isoprenoidal dialkyl glycerol diethers in cold-seep carbonate crusts. *Organic Geochemistry* **32**, 695-707 (2001).
27. B. D. A. Naafs, J. Blewett, R. D. Pancost, Bacterial diether lipids as a novel proxy to reconstruct past changes in sedimentary oxygenation. *Geochimica et Cosmochimica Acta*, (2025).
28. N. Yamauchi, The Pathway of Leucine to Mevalonate in Halophilic Archaea: Efficient Incorporation of Leucine into Isoprenoidal Lipid with the Involvement of Isovaleryl-CoA Dehydrogenase in Halobacterium salinarum. *Bioscience, Biotechnology, and Biochemistry* **74**, 443-446 (2010).
29. N. Yamauchi, R. Tanoue, Deuterium incorporation experiments from (3R)- and (3S)-[3-2H]leucine into characteristic isoprenoidal lipid-core of halophilic archaea suggests the involvement of isovaleryl-CoA dehydrogenase. *Bioscience, Biotechnology, and Biochemistry* **81**, 2062-2070 (2017).
30. S. Jain, A. Caforio, A. J. M. Driessen, Biosynthesis of archaeal membrane ether lipids. *Frontiers in Microbiology* **Volume 5 - 2014**, (2014).
31. A. Huguet, T. B. Meador, F. Laggoun-Défarge, M. Könneke, W. Wu, S. Derenne, K.-U. Hinrichs, Production rates of bacterial tetraether lipids and fatty acids in peatland under varying oxygen concentrations. *Geochim. Cosmochim. Acta* **203**, 103-116 (2017).
32. X.-L. Liu, D. Birgel, F. J. Elling, P. A. Sutton, J. S. Lipp, R. Zhu, C. Zhang, M. Könneke, J. Peckmann, S. J. Rowland, R. E. Summons, K.-U. Hinrichs, From ether to acid: A plausible degradation pathway of glycerol dialkyl glycerol tetraethers. *Geochimica et Cosmochimica Acta* **183**, 138-152 (2016).
33. J. S. Hingley, C. C. Martins, C. Walker-Trivett, J. K. Adams, S. Naeher, C. Häggi, S. J. Feakins, B. D. A. Naafs, The global distribution of Isoprenoidal Glycerol Dialkyl Diethers (isoGDDs) is consistent with a predominant degradation origin. *Organic Geochemistry* **192**, 104782 (2024).

34. J. W. Weijers, S. Schouten, E. C. Hopmans, J. A. Geenevasen, O. R. David, J. M. Coleman, R. D. Pancost, J. S. Sinninghe Damsté, Membrane lipids of mesophilic anaerobic bacteria thriving in peats have typical archaeal traits. *Environ. Microbiol.* **8**, 648-657 (2006).
35. B. Chappe, P. Albrecht, W. Michaelis, Polar Lipids of Archaebacteria in Sediments and Petroleums. *Science* **217**, 65-66 (1982).
36. J. S. Sinninghe Damsté, E. C. Hopmans, R. D. Pancost, S. Schouten, J. a. J. Geenevasen, Newly discovered non-isoprenoid glycerol dialkyl glycerol tetraether lipids in sediments. *ChemComm*, 1683-1684 (2000).
37. J. S. Sinninghe Damsté, W. I. Rijpstra, E. C. Hopmans, J. W. Weijers, B. U. Foesel, J. Overmann, S. N. Dedysh, 13,16-Dimethyl octacosanedioic acid (iso-diabolic acid), a common membrane-spanning lipid of Acidobacteria subdivisions 1 and 3. *Appl. Environ. Microbiol* **77**, 4147–4154 (2011).
38. V. Schneider, J. M. W. Antoszkiewicz, M. Vreeken, S. M. K. Cheung, Z. Zeng, D. A. Atencio, A. V. Gallego-Sala, J. Blewett, R. D. Pancost, B. D. A. Naafs, Environmental indications and controls of bacterial membrane lipids in a tropical peatland from Panama. *Organic Geochemistry* **210**, 105094 (2025).
39. E. C. Hopmans, J. W. H. Weijers, E. Schefuß, L. Herfort, J. S. Sinninghe Damsté, S. Schouten, A novel proxy for terrestrial organic matter in sediments based on branched and isoprenoid tetraether lipids. *EPSL* **224**, 107-116 (2004).
40. F. Peterse, J. Van Der Meer, S. Schouten, J. W. H. Weijers, N. Fierer, R. B. Jackson, J.-H. Kim, J. S. Sinninghe Damsté, Revised calibration of the MBT–CBT paleotemperature proxy based on branched tetraether membrane lipids in surface soils. *Geochim. Cosmochim. Acta* **96**, 215-229 (2012).
41. S. Schouten, E. C. Hopmans, J. S. Sinninghe Damsté, The organic geochemistry of glycerol dialkyl glycerol tetraether lipids: A review. *Org. Geochem.* **54**, 19-61 (2013).
42. J. Li, R. D. Pancost, B. D. A. Naafs, H. Yang, C. Zhao, S. Xie, Distribution of glycerol dialkyl glycerol tetraether (GDGT) lipids in a hypersaline lake system. *Org. Geochem.* **99**, 113-124 (2016).
43. P. Galliker, O. Grather, M. Riimmler, W. Fitz, D. Arigoni, in *Vitamin B12 and B12-Proteins*. (1998), pp. 447-458.
44. M. Fontecave, M. Atta, E. Mulliez, S-adenosylmethionine: nothing goes to waste. *Trends Biochem. Sci.* **29**, 243-249 (2004).
45. P. Gong, P. Lei, S. Wang, A. Zeng, H. Lou, Post-Translational Modifications Aid Archaeal Survival. *Biomolecules* **10**, 584 (2020).
46. L. Lauinger, P. Kaiser, Sensing and Signaling of Methionine Metabolism. *Metabolites* **11**, (2021).
47. A. A. Garcia, G. L. Chadwick, X. L. Liu, P. V. Welander, Identification of two archaeal GDGT lipid-modifying proteins reveals diverse microbes capable of GMGT biosynthesis and modification. *Proc. Natl. Acad. Sci. USA* **121**, e2318761121 (2024).
48. S. J. Mentch, J. W. Locasale, One-carbon metabolism and epigenetics: understanding the specificity. *Ann N Y Acad. Sci.* **1363**, 91-98 (2016).
49. S. Zhou, L. M. Alkhalaf, E. L. C. De Los Santos, G. L. Challis, Mechanistic insights into class B radical-S-adenosylmethionine methylases: ubiquitous tailoring enzymes in natural product biosynthesis. *Curr. Opin. Chem. Biol.* **35**, 73-79 (2016).
50. Q. Zhang, W. A. Van Der Donk, W. Liu, Radical-Mediated Enzymatic Methylation: A Tale of Two SAMS. *Acc. Chem. Res.* **45**, 555-564 (2012).
51. T. Q. Nguyen, Y. Nicolet, Structure and Catalytic Mechanism of Radical SAM Methylases. *Life (Basel)* **12**, (2022).
52. F. J. Elling, F. Pierrel, S.-C. Chobert, S. S. Abby, T. W. Evans, A. Reveillard, L. Pelosi, J. Schnoebelen, J. D. Hemingway, A. Boumendjel, K. W. Becker, P. Blom, J. Cordes, V. Nathan, F. Baymann, S. Lücker, E. Spieck, J. R. Leadbetter, K.-U. Hinrichs, R. E. Summons, A. Pearson, A novel quinone biosynthetic pathway illuminates the evolution of aerobic metabolism. *Proceedings of the National Academy of Sciences* **122**, e2421994122 (2025).
53. F. J. Elling, J. D. Hemingway, T. W. Evans, J. J. Kharbush, E. Spieck, R. E. Summons, A. Pearson, Vitamin B₁₂-dependent biosynthesis ties amplified 2-methylhopanoid

production during oceanic anoxic events to nitrification. *Proceedings of the National Academy of Sciences* **117**, 32996-33004 (2020).
54. C. D. Rosendahl, X. Zhao, A. E. Maloney, J. M. Mcfarlin, K. J. Keller, R. Kreutz, J. Altun, L. H. Bachmann, J. Hartmann, H. K. Batther, A. N. Calhoun, M. Elvert, A. Pearson, W. D. Leavitt, S. H. Kopf, F. J. Elling, Improved procedures for the cleavage and reduction of GDGTs for hydrogen isotope analysis. *Organic Geochemistry* **218**, 105139 (2026).
55. R. S. Cahn, C. K. Ingold, V. Prelog, The specification of asymmetric configuration in organic chemistry. Experientia 12, 81-94 (1956).
56. R. S. Cahn, C. K. Ingold, V. Prelog, Specification of Molecular Chirality. Angewandte Chemie 5, 385-415 (1966).

Acknowledgments
We thank the European Organization of Organic Geochemistry (EAOG) for awarding me, V. Schneider, as a candidate for receiving the EAOG research award which provided the opportunity to work together with Sebastian Kopf at the University of Colorado, Boulder. The authors wish to thank the NERC for partial funding of the National Environmental Isotope Facility (NEIF; contract no. NE/Y005449/1), the European Research Council under the European Union's Seventh Framework Programme (FP/2007-2013) and European Research Grant Agreement number 340923 for funding GC-MS capabilities, as well as the US National Science Foundation which contributed to funding the work at the University of Colorado Boulder via a CAREER grant to S. Kopf (EAR-1945484). We also would like to acknowledge the laboratory infrastructure provided by the GeoMicrobial Co-Culturing (GEOM) Core Facility at University of Colorado Boulder (RRID:SCR_025034) which provided the infrastructure for our culturing experiments and the CU Boulder Earth Systems Stable Isotope Lab (CUBES-SIL) Core Facility (RRID:SCR_019300) which provided analytical infrastructure. F. Elling acknowledges funding by the Deutsche Forschungsgemeinschaft (grant # 441217575). A. Winter want to thank the Biotechnology and Biological Sciences Research Council (BBSRC) for funding (BB/W008823/1). Besides our funders, we also like to thank R. Pancost and M. Crump for their expertise and support during this project.

Funding:
Vivien Schneider: Royal Society, University of Bristol, NEIF Facility, EAOG Research Award
Catherine Fontana: GeoMicrobial Co-Culturing (GEOM) Core Facility, National Science Foundation
Ashley J. Winter: Biotechnology and Biological Sciences Research Council (BBSRC)
Adam D. Younkin: University of Colorado Boulder, National Science Foundation
Felix J. Elling: Deutsche Forschungsgemeinschaft
B. David A. Naafs: Royal Society, University of Bristol, NEIF Facility,
Sebastian H. Kopf: University of Colorado Boulder

Contribution:
Conceptualization: VS, FE, SK, BDAN
Methodology: AJW, VS, CF, ADJ
Investigation: VS, BDAN, SK, AJW
Visualization: VS
Supervision: SK, BDAN
Writing—original draft: VS, BDAN
Writing—review & editing: VS, BDAN, FE, SK, AJW

Competing interests: Authors declare that they have no competing interests.

Figures and Tables

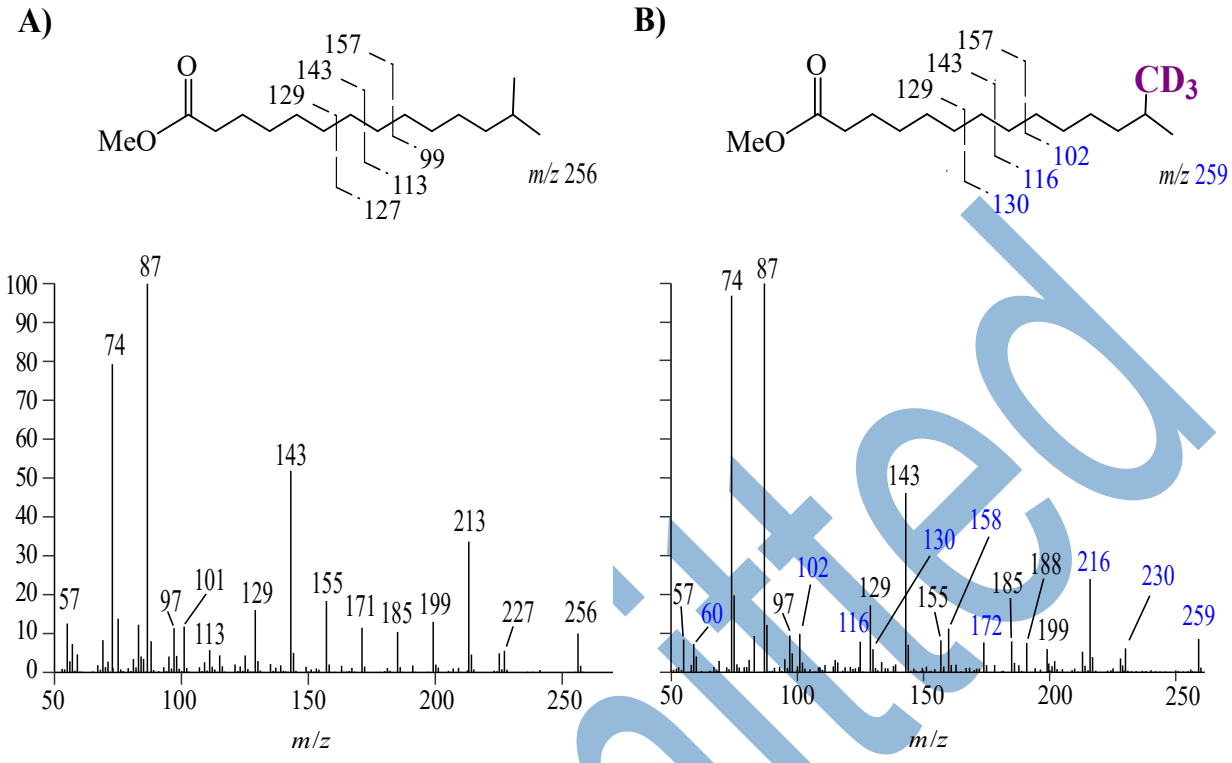

Figure 1: *Mass spectrum of iso$C_{15:0}$ fatty acid methyl ester from a control culture (A) and CD_3 L-Leucine spiked experiment (B), which shows mass shift of 3 amu in blue (note that either terminal (bridging) methyl group could be the labelled one).*

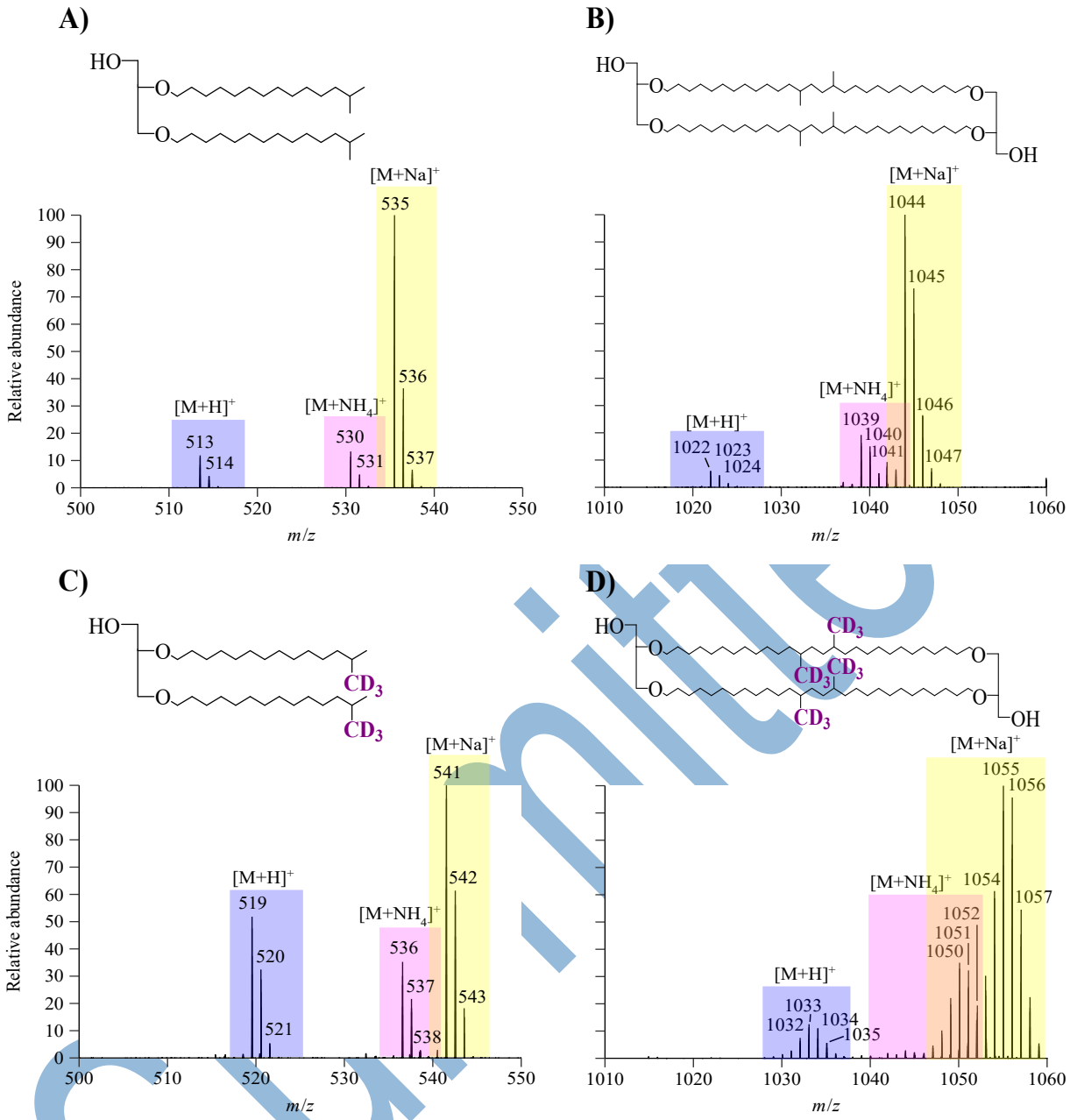

Figure 2: *MS1 mass spectrum of the control (A, B) and CD_3 labeled $isoC_{15:0}$ DEG (C) and brGDGT-Ia from spiked experiment (D). The different adducts are color coded; protonated mass (blue), ammoniated mass (pink) and sodiated mass (yellow). The expected mass shift of +6 amu for the $isoC_{15:0}$ DEG (C) and +12 amu for the brGDGT-Ia in the spiked experiment (D) is visible in all formed adducts. For further information regarding the fragmentation pattern please refer to the supplementary information; text, fig. S7 and fig. S8.*

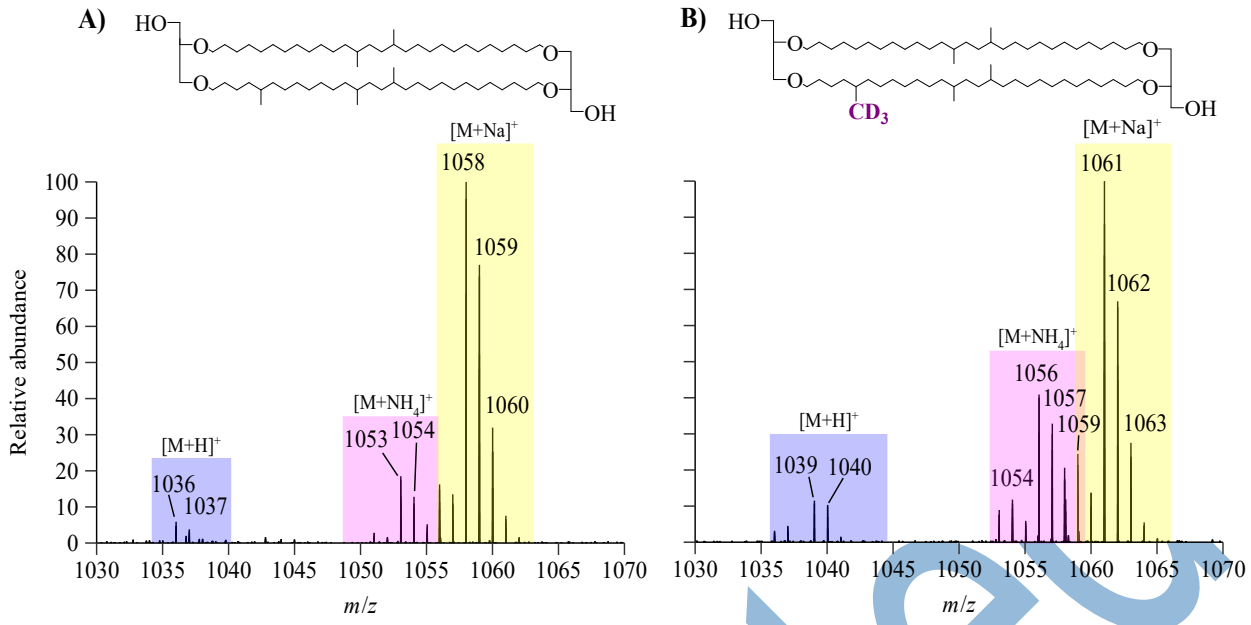

Figure 3: *MS1 of brGDGT-IIa from the control experiment (A) and the spiked L-methionine experiment (B). The different adducts are color coded; protonated mass (blue), ammoniated mass (pink) and sodiated mass (yellow). The expected mass shift of +3 amu in the spiked experiment is visible in all formed adducts.*

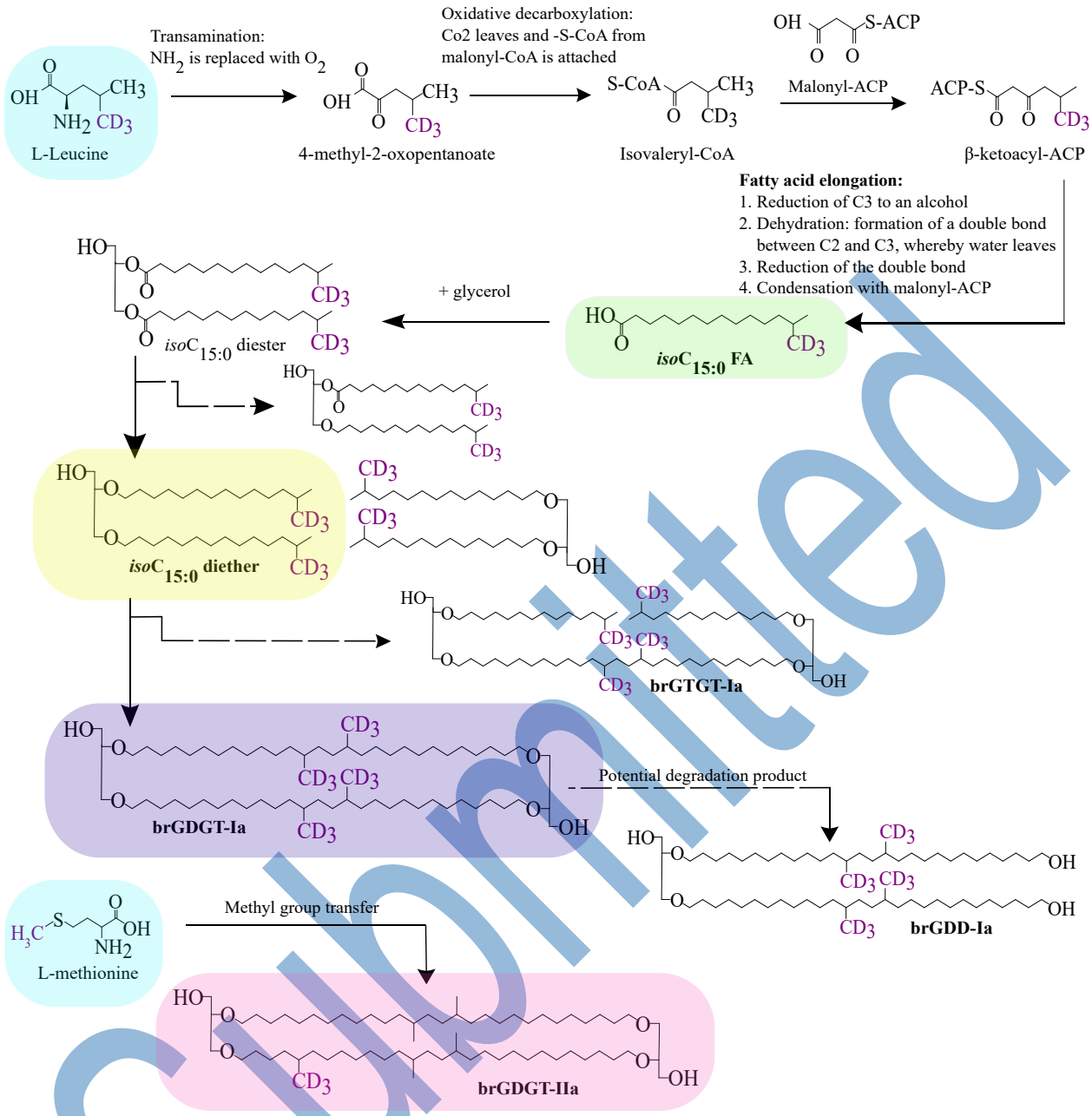

Figure 4: *Confirmed biosynthetic pathway of tetra- (Ia) and pentamethylated (IIa) brGDGT in the bacterium S. usitatus, starting with (labeled) L-Leucine. The additional methylation occurs after the formation of a brGDGT likely through a class B radical SAM mechanism (mechanisms based on the additional methyl shown to originate from the amino acid L-methionine) (49). Colored areas highlight key lipids.*